Acta Pharmacologica Sinica (2017) 38: 699–709
 1671-4083/17
www.nature.com/aps

Original Article

Sarsasapogenin-AA13 inhibits LPS-induced inflammatory responses in macrophage cells *in vitro* and relieves dimethylbenzene-induced ear edema in mice

Dong DONG, Nan-nan ZHOU, Rui-xuan LIU, Jia-wei XIONG, Hui PAN, Si-qi SUN, Lei MA*, Rui WANG*

Shanghai Key Laboratory of New Drug Design, School of Pharmacy, East China University of Science and Technology, Shanghai 200237, China

Abstract

Sarsasapogenin-AA13 (AA13) is a novel synthetic derivative of sarsasapogenin extracted from the Chinese herb Rhizoma Anemarrhenae. In this study we investigated the effects of AA13 on lipopolysaccharide (LPS)-induced production of inflammatory factors in macrophage cells and the anti-inflammatory activity of AA13 in an inflammatory model of dimethylbenzene-induced ear edema. Macrophage cells (RAW264.7 cells and mouse peritoneal macrophages) were exposed to LPS (1 μg/mL); pretreatment with AA13 (5–20 μmol/L) dose-dependently inhibited LPS-induced production of NO, TNF-α and PGE_2, and LPS-stimulated expression levels of COX-2 and iNOS. Furthermore, pretreatment with AA13 dose-dependently suppressed LPS-stimulated phosphorylation of p38 and JNK, but had no effect on ERK in RAW264.7 cells. Moreover, pretreatment with AA13 inhibited LPS-induced activation of the nuclear factor (NF)-κB in RAW264.7 cells. The *in vivo* anti-inflammatory activity of AA13 was demonstrated in a mouse inflammatory model: pre-treatment with either AA13 (20 $mg \cdot kg^{-1} \cdot d^{-1}$, ig) or a positive control antifani (10 $mg \cdot kg^{-1} \cdot d^{-1}$, ig) for 3 d significantly relieved dimethylbenzene-induced ear edema. Our results demonstrate that AA13 effectively inhibit LPS-induced inflammatory responses in macrophage cells *in vitro* and relieve dimethylbenzene-induced ear edema *in vivo*.

Keywords: sarsasapogenin; AA13; antifani; anti-inflammation; inflammatory factor; nuclear factor-κB; mitogen-activated protein kinases; ear edema

Acta Pharmacologica Sinica (2017) 38: 699–709; doi: 10.1038/aps.2016.180; published online 27 Feb 2017

Introduction

Inflammation is a complex biological process mediated by the activation of inflammatory or immune cells, which is a response to infection and antigens[1]. The inflammatory process is helpful to eliminate pathogens and to repair damaged tissue, which may be one mechanism of protective immunity[2]. However, superabundant pro-inflammatory cytokines may lead to secondary tissue injury, and excessive inflammatory responses may accelerate or cause the development of neurodegeneration and cancer[3, 4]. Under inflammatory conditions, macrophages play a central role in the activation of inflammatory mediators and the overproduction of pro-inflammatory cytokines[1, 5].

Lipopolysaccharide (LPS) is a characteristic component of the outer membrane of Gram-negative bacteria[6]. During Gram-negative bacterial infections, a series of cytokines that play important roles in the pathogenesis of anti-cancer, antibacterial, and anti-viral immune responses are synthesized and released[7, 8]. LPS can stimulate many types of cells, macrophages and neutrophils, for instance, to release pro-inflammatory mediators and cytokines such as interleukin-6 (IL-6), tumor necrosis factor-α (TNF-α), inducible nitric oxide synthase (iNOS) and cyclooxygenase-2 (COX-2)[9–11]. Nuclear factor (NF)-κB signaling and translocation are the key actions in inflammatory reactions[12]. In normal cells, NF-κB is located in the cytoplasm and complexed with the inhibitory protein IκBa. The phosphorylation of IκBα results in its dissociation from NF-κB. With the degradation of IκBα, the NF-κB is released from the complex and translocated to the nucleus where it can 'turn on' the expression of specific genes, which leads to the transcription of pro-inflammatory signaling effectors[13].

*To whom correspondence should be addressed.
E-mail ruiwang@ecust.edu.cn (Rui WANG)
malei@ecust.edu.cn (Lei MA)
Received 2016-07-31 Accepted 2016-12-05

Furthermore, there is considerable evidence that NF-κB can increase the expression of iNOS and COX-2. Many studies have demonstrated the downregulation of the NF-κB pathway in anti-inflammatory processes[14, 15]. C-Jun N-terminal kinases (JNKs) belong to the MAPK family and are responsive to stress stimuli induced by LPS[16]. They also play a role in the cellular apoptosis pathway and in the activation of inflammatory cytokines through regulating transcription factors[17, 18].

Rhizoma Anemarrhenae is widely used as a traditional Chinese herb and is known to have anti-diabetic and diuretic effects[19, 20]. We have previously found that a derivative of sarsasapogenin, an active ingredient in Rhizoma Anemarrhenae, is effective in an animal model of in ameliorating memory deficits associated with aging (BMCL, in press). Moreover, the density of muscarinic acetylcholine receptors in the brains increased after sarsasapogenin treatment, which might contribute to the nootropic effect[21, 22]. Timosaponin ameliorates learning and memory deficits in mice, mainly by inhibiting acetylcholinesterase (AChE)[23]. Anemarsaponin B, a steroid saponin isolated from Rhizoma Anemarrhenae, was demonstrated to have anti-inflammatory effects in LPS-stimulated RAW264.7 macrophages, and anemarsaponin B significantly decreased the levels of iNOS, COX-2 and pro-inflammatory cytokines[24]. AA13 is a novel synthetic derivative of sarsasapogenin. We have previously found that AA13 is the most effective sarsasapogenin derivative in LPS-induced inflammation (unpublished, data not shown). In this study, we will further investigate the anti-inflammatory effects and the possible anti-inflammatory mechanisms of AA13.

Materials and methods

Drugs and reagents

3-(4,5-Dimethythiazol-2-yl)-2,5-diphenyl-tetrazolium bromide (MTT) and an electrochemiluminescence (ECL) reagent kit were obtained from Sangon Biotech (Shanghai, China). Lipopolysaccharide (LPS) was obtained from Sigma-Aldrich (St Louis, MO, USA). Dulbecco's modified Eagle's medium (DMEM) was purchased from Hyclone (Logan, UT, USA). Fetal bovine serum (FBS) was obtained from Gibco (Grand Island, NY, USA). Prostaglandin E2 EIA kits were from Cayman Chemicals (Ann Arbor, MI, USA). Rabbit anti-phospho-Akt (Ser478) and Akt, rabbit anti-phospho-Erk1/2 (Thr202/Tyr204) and Erk1/2, rabbit anti-phospho-p38 (Thr180/Thy182) and p38, rabbit anti-phospho-JNK (Thr183/Tyr185) and JNK, and NF-κB were provided by Cell Signaling Technology (Boston, MA, USA). Rabbit anti-phospho-IκB was obtained from Abcam Trading (Shanghai) Company Ltd (Pudong, Shanghai, China). Secondary antibodies were purchased from Santa Cruz Biotechnology, Inc (Santa Cruz, CA, USA).

AA13 (Figure 1) was provided by Lei MA's lab at the School of Pharmacy, East China University of Science and Technology. The purity of the synthetic AA13 was 98%. For all experiments, AA13 was freshly dissolved in DMSO and diluted with the media for cell culture. AA13 was synthesized by the following method: 4-nitrophenyl chloroformate (6 mmol) was slowly added to a mixture of the sarsasapogenin (1.664 g, 4 mmol) and pyridine (0.5 mL) in dichloromethane under an argon gas atmosphere at zero temperature. Then, the mixture was stirred at room temperature for four hours. The reaction mixture was quenched with water (100 mL), and the product was extracted with dichloromethane (3×100 mL). Then, the organic phase was dried (sodium sulfate) and concentrated. Column chromatography was used to purify the sample. Consequently, intermediate S (2.19 g) was obtained. Intermediate S (58.1 mg, 0.1 mmol) and triethylamine (0.05 mL) were mixed in dichloromethane under an argon gas atmosphere at zero temperature. Isobutylamine (0.15 mmol) was slowly added. Then, the mixture was stirred at room temperature for three hours. The reaction mixture was quenched with water (30 mL), and the product was extracted with dichloromethane (3×30 mL). Then, the organic phase was dried (sodium sulfate) and concentrated. Column chromatography was used to purify the sample. Then, white solid AA13 was obtained (purity 98%). ^{1}H NMR (400 MHz, $CDCl_3$) δ 4.99 (s, 1H), 4.70 (s, 1H), 4.43 (dd, *J*=14.3, 7.3 Hz, 1H), 3.97 (d, *J*=10.6 Hz, 1H), 3.32 (d, *J*=10.9 Hz, 1H), 3.02 (t, *J*=6.3 Hz, 2H),1.12–2.12 (m, 27H), 1.10 (d, *J*=7.0 Hz, 3H), 1.01 (m, 6H), 0.94 (s, 3H), 0.93 (s, 3H), 0.78 (s, 3H). MS (ESI): *m/z* 516.45 $[M+H]^+$; HRMS (ESI): *m/z* $[M+H]^+$ Calcd for $C_{32}H_{53}NO_4$: 516.1301; Found: 516.1308.

Animals

Male ICR mice (10 weeks old, 30±3 g) were provided by Shanghai Sippr-bk Laboratory Animal Co, Ltd (Shanghai, China). The environment was climate-controlled with a 12 h light/12 h dark cycle, and water and food were provided. The certificate number of the animal breeder was 14121496 of the Shanghai Laboratory Animal Staff. All experimental procedures were performed in accordance with the National Institutes of Health Guide for the Care and Use of Laboratory Animals in Shanghai, China, and in compliance with the

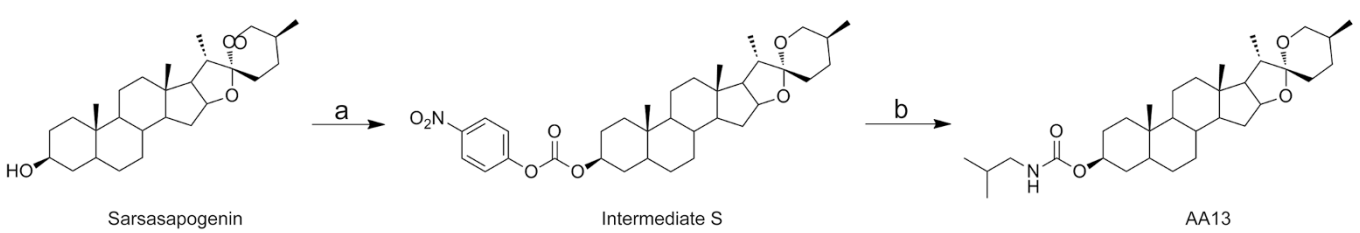

Figure 1. Synthesis of AA13. Reagents and conditions: (a) 4-Nitrophenyl chloroformate, pyridine, DCM, room temperature.; (b) Isobutylamine, triethylamine, DCM, room temperature.

Agreement of the Ethics Committee on Laboratory Animal Care of the East China University of Science and Technology.

Cell culture

RAW264.7 cells (Type Culture Collection of the Chinese Academy of Sciences, Shanghai, China) were cultured in DMEM medium supplemented with 10% FBS and were kept at 37 °C in humidified 5% CO_2 and 95% air. Cells were seeded in cell culture plates (Jet Bio-Filtration Products Co, Ltd, Guangzhou, China) at a density of 1×10^5/mL before experiments. The experiments were carried out 24 h after cells were seeded.

The ICR mice were sacrificed and doused in 75% alcohol for 5 min. Peritoneal macrophages were harvested by lavaging with chilled RPMI-1640 medium supplemented with 10% FBS, penicillin (100 U/mL) and streptomycin (100 U/mL). The resident macrophages were washed three times and were seeded in 96-well cell culture plates at a density of 1×10^6/mL. After 2 h incubation at 37 °C and an atmosphere of 5% CO_2, the nonadherent cells were removed by washing with medium.

MTT assay

The mitochondrial-dependent reduction of MTT to formazan was used to determine cell viability[25]. RAW264.7 cells were seeded in a 96-well plate at a density of 5×10^5 cell/mL. After 24 h, AA13 was added at the indicated concentrations (5, 10, 15, and 20 μmol/L). Peritoneal macrophages plated at a density of 1×10^6 /well in a 96-well plate, and AA13 was added at the indicated concentrations (5, 10, 15, and 20 μmol/L). Cell viability was measured after another 24 h incubation. Then, 10 μL of MTT (5 mg/mL) was added to the wells, and the cells were incubated for another 4 h at 37 °C. The supernatants were removed carefully, and 100 μL of DMSO was added to dissolve the formazan. The absorbance of each group was measured using a Synergy 2 Multi-Mode Microplate Reader (BioTek, Winooski, VT, USA) at a wavelength of 490 nm. The untreated cells were considered as 100% of the viable cells, and the results are expressed as the percentage of viable cells compared with the untreated cells.

Nitrite measurement

RAW264.7 macrophage cells plated at a density of 1×10^5/well in a 96-well plate were treated in serum-free medium for 12 h. Cells were pretreated with AA13 (5, 10, 15, and 20 μmol/L) for 30 min, followed by LPS (1 μg/mL) stimulation for 24 h without removing AA13. Peritoneal macrophages were plated at a density of 1×10^6/well in a 96-well plate and pretreated with AA13 (5, 10, 15, and 20 μmol/L) for 30 min, followed by LPS (1 μg/mL) stimulation for 24 h without removing the AA13. Suspended media was collected to measure the nitrite concentrations as an indicator of NO production according to the Griess reaction[26].

PGE_2 and TNF-α measurement

RAW264.7 macrophage cells plated at a density of 1×10^5/well in a 12-well plate were treated in serum-free medium for 12 h. Cells were pretreated with AA13 (5, 10, 15, and 20 μmol/L) for 30 min, followed by LPS (1 μg/mL) stimulation for 24 h, without removing the AA13. The cell culture supernatants were harvested and centrifuged at 5000×*g* for 10 min. TNF-α and PGE_2 levels were measured using the TNF-α and PGE_2 EIA kits according to the manufacturer's directions.

Western blot analysis for MAPKs, iNOS, COX-2 p-IκB, and NF-κB

After the treatment with LPS (1 μg/mL) in the presence or absence of AA13 (5, 10, 15, and 20 μmol/L) for 30 min, RAW264.7 cells were washed three times with cold D-Hank's solution (137.93 mmol/L NaCl, 5.33 mmol/L KCl, 4.17 mmol/L $NaHCO_3$, 0.441 mmol/L KH_2PO_3, 0.338 mmol/L Na_2HPO_4) and lysed in a cold lysis buffer (50 mmol/L Tris-HCl, 1.0 mmol/L EDTA, 150 mmol/L NaCl, 0.1% SDS, 1% sodium deoxycholate, 1 mmol/L PMSF) containing a cocktail of protease inhibitors and phosphatase inhibitors. The proteins (40 μg) were separated by SDS-PAGE and transferred to polyvinylidene fluoride (PVDF) membranes. The target proteins were probed with primary and secondary antibodies, and immunoreactive bands were detected using the Tanon5200S Chemiluminescence Imaging System (Tanon, Shanghai, China). Protein bands were quantified by densitometric analysis using Image J (version 1.45s, NIH, USA)[27].

Immunocytochemistry

RAW264.7 macrophage cells plated at a density of 1×10^4/well were treated in serum-free medium for 12 h. Then, the cells were pretreated with AA13 (20 μmol/L) for 30 min, followed by LPS stimulation for 1 h. After a wash with PBS, cells were fixed with 4% paraformaldehyde (PFA) solution for 15 min at room temperature. Cells were then washed with PBS again and permeabilized with 0.1% Triton-X100 for 30 min at room temperature. After 1 h blocking with 5% BSA at room temperature, the cells were incubated with NF-κB p65 primary antibody (1:50 dilutions) at 4 °C overnight. Alexa Fluor 546 goat anti-rabbit IgG (H+L) secondary antibody (Invitrogen, 1:4000) was added to the cells and incubated for 2 h at room temperature after three washes with PBS. For nuclear staining, a DAPI solution was added at a concentration of 0.1 μg/mL and incubated for 10 min in the dark. The cell images were acquired under a confocal microscope (Nikon, A1R, Japan) at 200× magnification[28].

NF-κB p65 detection in subcellular compartments

After being cultured in serum-free medium for 12 h, the cells were pretreated with AA13 (5, 10, 15, and 20 μmol/L) for 30 min, followed by LPS (1 μg/mL) stimulation for another 1 h without removing AA13. The treated cells were washed with PBS and suspended in lysis buffer A (10 mmol/L HEPES, pH 7.6; 10 mmol/L KCl, 1 mmol/L dithiothreitol, 0.1 mmol/L EDTA and 0.5 mmol/L PMSF) for 10 min on ice. Cytosolic fractions were separated using pipettes after centrifugation at 12 000×*g* for 10 min at 4 °C. The remaining unclear fractions were lysed again with lysis buffer B (20 mmol/L HEPES, pH 7.6; 1 mmol/L EDTA, 1 mmol/L DTT, 0.5 mmol/L PMSF, 25%

glycerol and 0.4 mol/L NaCl) and centrifuged at 12000×*g* for 20 min. As mentioned above, anti-NF-κB p65 (1:1000 dilution) primary antibody was used to detect the cytosolic and nuclear proteins by western blotting. GAPDH and PCNA were used as internal controls for the cytoplasmic and nuclear fractions[29].

Dimethylbenzene-induced mouse ear edema

Mice were randomly assigned to three groups (n=5), and each group of mice was intragastrically (ig) administered sterile physiological saline (model groups), antifani (10 mg/kg) or AA13 (20 mg/kg) once a day for three days. Ear edema was induced by smearing dimethylbenzene (40 μL/ear) on the inner and outer surfaces of the right ear 1 h after the last administration of AA13 and antifani. Ear punches (6 mm diameter) were removed from both the right and left ears at the same location. The weight difference of ear punches between the right and left ears of the same mouse was measured. For histological analysis, ear tissues were fixed in 4% paraformaldehyde, dehydrated with sucrose solution, and embedded in optimum cutting temperature compound. Frozen sections (10 mm) were stained with hematoxylin and eosin and observed under a Nikon optical microscope.

Statistical analysis

All data were expressed as the mean±SEM. Commercially available SPSS version 15.0 was used to assess the statistical significance. The data analysis was performed using one-way analysis of variance (ANOVA) followed by a *post hoc* (Student-Newman-Keuls) test for multiple comparisons. A P value of <0.05 was considered significant.

Results

AA13 inhibited NO production in LPS-stimulated RAW264.7 cells and peritoneal macrophages

The MTT assay showed that AA13 did not exhibit cytotoxicity toward RAW264.7 cells at the concentrations of 5, 10, 15, and 20 μmol/L (Figure 2A). To investigate whether AA13 could affect LPS-induced NO production, RAW246.7 cells were pretreated with AA13 (5, 10, 15, and 20 μmol/L) for 30 min, followed by LPS (1 μg/mL) stimulation for 24 h without removing AA13. As shown in Figure 2B, AA13 at concentrations of 20, 15, and 10 μmol/L significantly reduced the production of NO in RAW264.7 cells in a dose-dependent manner. To verify these findings, peritoneal macrophages were pretreated with AA13 for 30 min, followed by LPS (1 mg/mL) stimulation for 24 h without removing the AA13. As shown in Figure 2C and Figure 2D, AA13 did not exhibit cytotoxicity toward peritoneal macrophages and could inhibit the NO production induced by LPS, which corresponded to experiments with RAW264.7 cells. The treatment of LPS and LPS plus AA13 had no cytotoxicity in cells that were used in

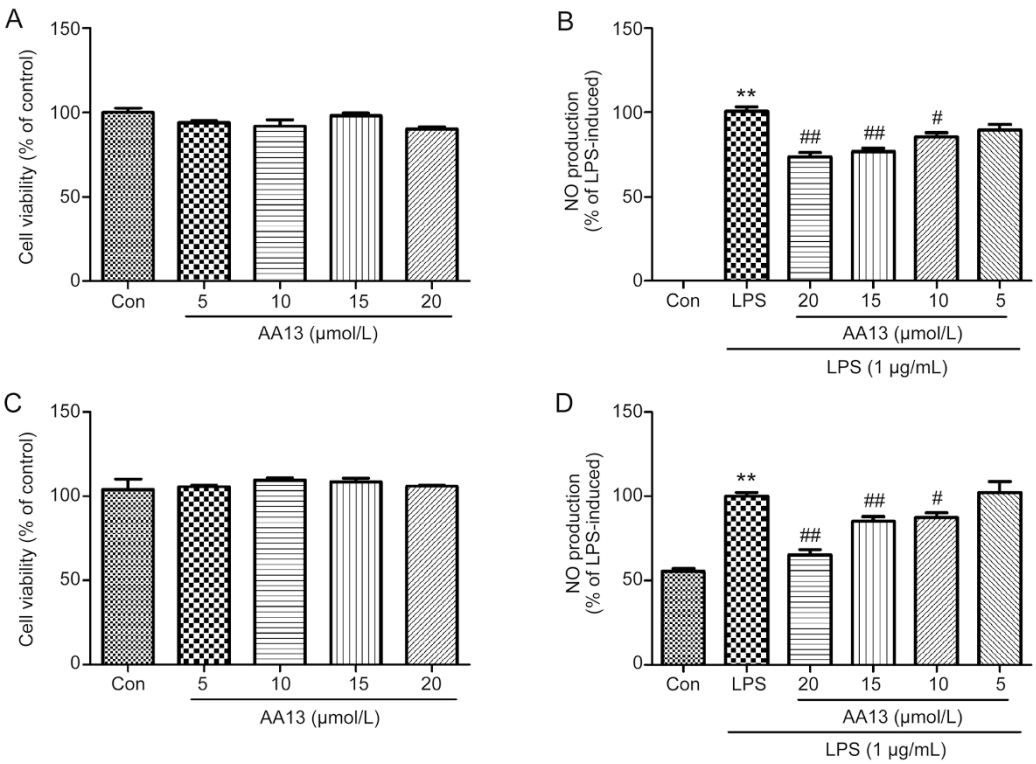

Figure 2. AA13 inhibited NO production in LPS-stimulated RAW264.7 cells and peritoneal macrophages. RAW264.7 (A) cells and peritoneal macrophages (C) were treated with AA13 for 24 h. Cell viability was determined by MTT assay. Cells were pretreated with AA13 for 30 min, followed by LPS (1 μg/mL) stimulation for 24 h. The NO production of RAW264.7 cells (B) and peritoneal macrophages (D) was measured by NO assay kit. n=3 for each group. Mean±SEM. $^{**}P$<0.01 *vs* control group. $^{\#}P$<0.05, $^{\#\#}P$<0.01 *vs* LPS-stimulated group.

the experiment (data not shown).

The effect of AA13 on pro-inflammatory cytokine production in LPS-stimulated RAW264.7 cells

To determine the effects of AA13 on the production of pro-inflammatory cytokines, RAW264.7 cells were pretreated with AA13 for 30 min, followed by LPS (1 μg/mL) stimulation for 24 h without removing the AA13. TNF-α and MCP-1 levels in the medium were measured by ELISA. As shown in Figure 3, LPS stimulation markedly increased the levels of TNF-α and MCP-1. Pretreatment with AA13 at 20 and 15 μmol/L significantly inhibited the increase of TNF-α, but had no effect on the levels of MCP-1.

AA13 inhibited LPS-stimulated PGE_2 production in RAW264.7 cells

Studies have found that the extracts of *Anemarrhenae asphodeloides* inhibited LPS-stimulated PGE_2 production in microglia[30]. To determine the effects of AA13 on the production of PGE_2, RAW264.7 cells were pretreated with AA13 for 30 min, followed by LPS (1 μg/mL) stimulation for 24 h without removing the AA13. PGE_2 level in the medium was measured by ELISA. As is shown in Figure 4, LPS stimulation markedly increased the level of PGE_2, and AA13 inhibited the production of PGE_2 in a dose-dependent manner.

The inhibition effect of AA13 on LPS-stimulated COX-2 and iNOS in RAW264.7 cells

To investigate whether the inhibitory effects of AA13 on NO, TNF-α and PGE_2 production are related to the regulation of the expression of COX-2 and iNOS, RAW264.7 cells were pretreated with AA13 for 30 min and then stimulated with LPS (1 μg/mL) for 1 h without removing the AA13. As shown in Figure 5, the levels of COX-2 and iNOS, determined by Western blot analysis, were significantly increased when the macrophages were treated with only LPS. The pretreatment of cells with AA13 at 20 and 15 μmol/L significantly reduced the levels of COX-2 and iNOS proteins in a dose-dependent manner.

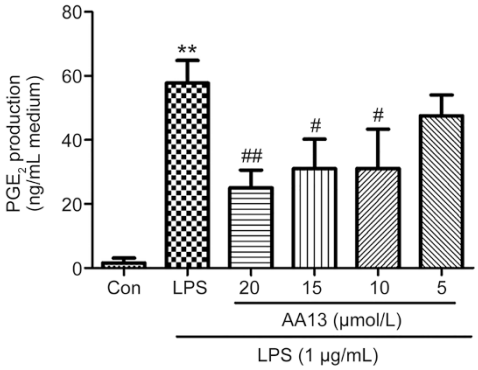

Figure 4. AA13 inhibited LPS-stimulated PGE_2 production in RAW264.7 cells (n=3 for each group). Cells were pretreated with AA13 for 30 min, followed by LPS (1 μg/mL) stimulation for 24 h. PGE_2 level in the medium was measured by ELISA. Mean±SEM. n=3 independent experiments. $^{**}P$<0.01 *vs* control group. $^{\#}P$<0.05, $^{\#\#}P$<0.01 *vs* LPS-stimulated group.

Effect of AA13 on the LPS-stimulated MAPK pathway in RAW264.7 cells

To confirm whether AA13 affects the activation of the MAPK signal pathway, RAW264.7 cells were pretreated with AA13 for 30 min, followed by LPS (1 μg/mL) stimulation for 1 h without removing AA13. The activation of MAPKs in cells was determined by Western blot. As shown in Figure 6, AA13 inhibited the LPS-stimulated phosphorylation of p38 and JNK at the concentrations of 15 and 20 μmol/L, but had no effect on ERK.

Effect of AA13 on LPS-stimulated NF-κB p65 translocation in RAW264.7 cells

To investigate the effect of AA13 on NF-κB p65 translocation, RAW264.7 cells were pretreated with AA13 for 30 min, followed by LPS (1 μg/mL) stimulation for 1 h without removing the AA13; the translocation of the p65 subunit of NF-κB was determined by immunochemistry. As shown in Figure 7, AA13 inhibited the LPS-induced transcriptional activation of

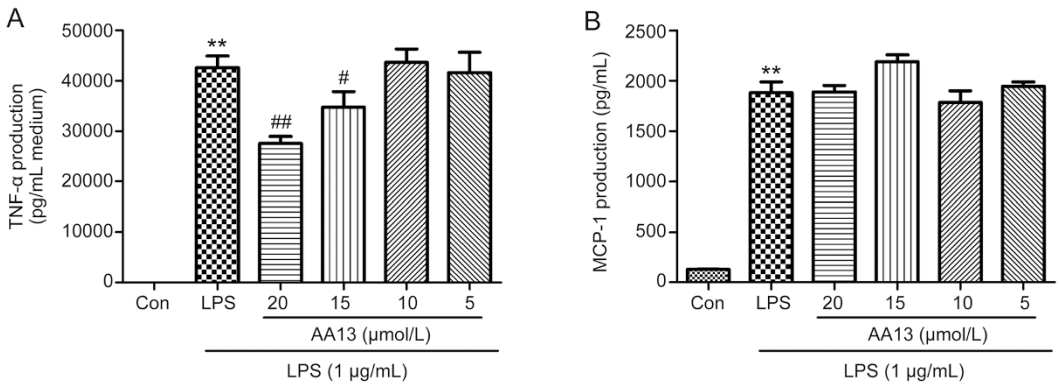

Figure 3. The effect of AA13 on pro-inflammatory cytokines production in LPS-stimulated RAW264.7 cells. RAW264.7 macrophage cells were pretreated with AA13 for 30 min, followed by LPS (1 μg/mL) stimulation for 24 h. TNF-α (A) and MCP-1 (B) level in the medium was measured by ELISA. Mean±SEM. n=3 independent experiments. $^{**}P$<0.01 *vs* control group. $^{\#}P$<0.05, $^{\#\#}P$<0.01 *vs* LPS-stimulated group.

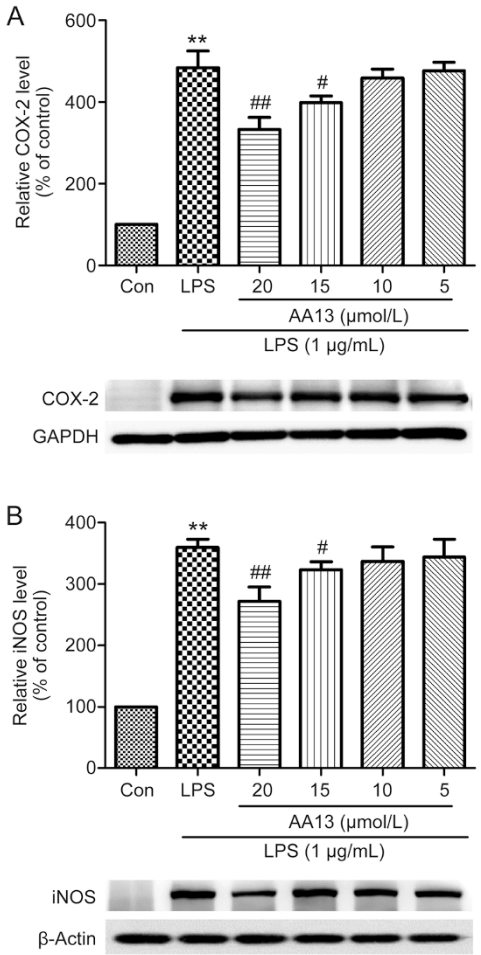

Figure 5. The inhibition effect of AA13 on LPS-stimulated COX-2 and iNOS in RAW264.7 cells (n=3 for each group). Cells were pretreated with AA13 for 30 min, followed by LPS (1 μg/mL) stimulation for 1 h. The level of COX-2 (A) and iNOS (B) were determined by Western blot. Mean±SEM. n=3 independent experiments. $^{**}P$<0.01 *vs* control group. $^{\#}P$<0.05, $^{\#\#}P$<0.01 *vs* LPS-stimulated group.

NF-κB. To confirm NF-κB activation, the protein level of p65 in the cytoplasm and nucleus were measured by Western blot. As the results show, the protein level of p65 in the cytoplasm (Figure 8A) was reduced by LPS treatment, while AA13 inhibited the reduction at concentrations of 20 and 15 μmol/L. Accordingly, with the change of p65 in the cytoplasm, the increase of p65 in the nucleus (Figure 8B) induced by LPS was inhibited by AA13. In addition, the phosphorylation of IκB (Figure 8C) was also inhibited by AA13.

AA13 inhibited dimethylbenzene-induced edema in mouse ears

The anti-inflammatory activity of AA13 was investigated using a dimethylbenzene-induced mouse ear edema model, which is commonly used in inflammatory experiments. After treatment with AA13 and following dimethylbenzene induction, the weight of 6 mm diameter ear samples was

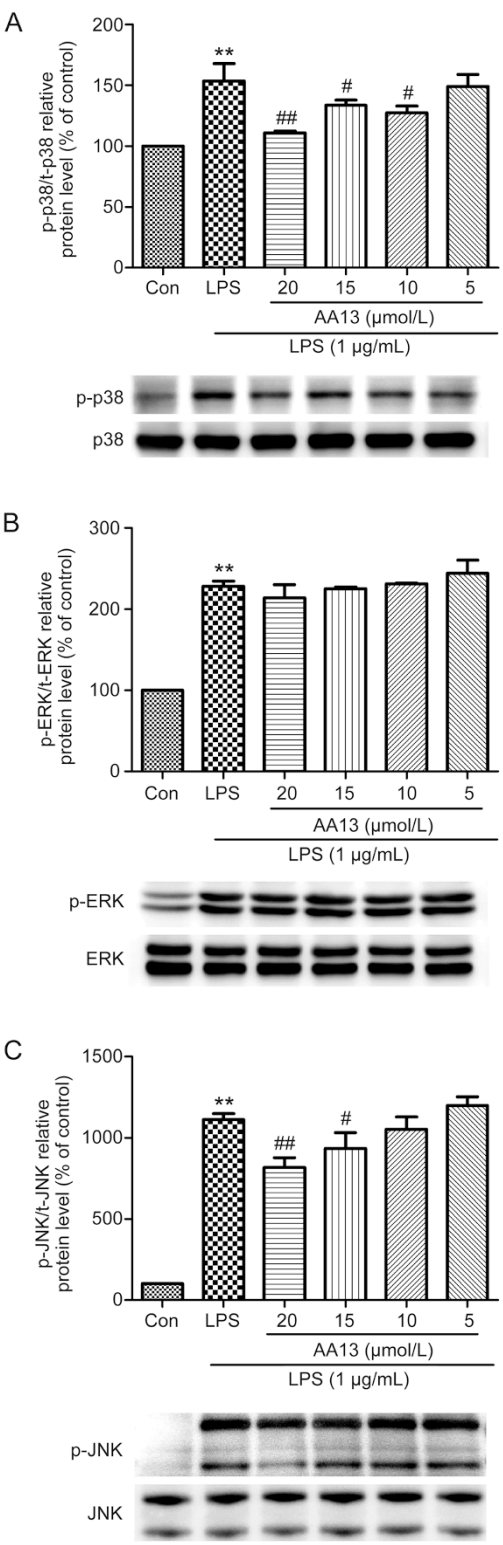

Figure 6. Effect of AA13 on LPS-stimulated MAPKs pathway in RAW264.7 cells (n=3 for each group). Cells were pretreated with AA13 for 30 min, followed by LPS (1 μg/mL) stimulation for 1 h. The level of p-p38/p38 (A), p-ERK/ERK (B) and p-JNK/JNK (C) were determined by Western blot. Mean±SEM. n=3 independent experiments. $^{**}P$<0.01 *vs* control group. $^{\#}P$<0.05, $^{\#\#}P$<0.01 *vs* LPS-stimulated group.

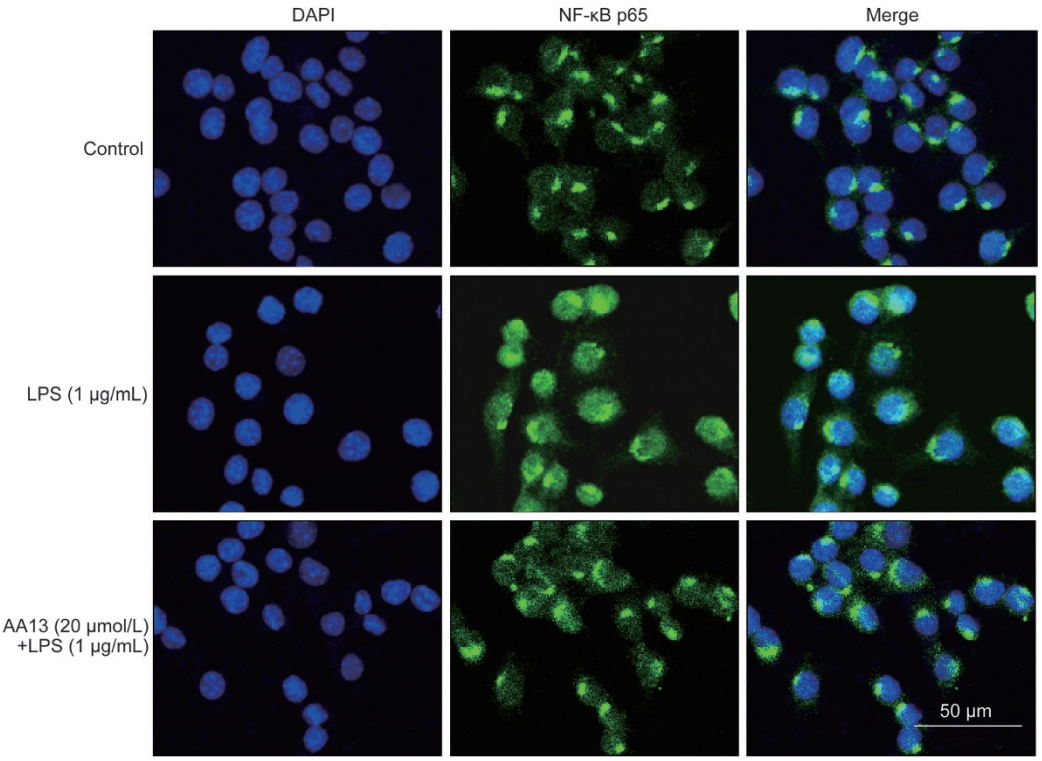

Figure 7. Effect of AA13 on LPS-stimulated NF-κB p65 translocation in RAW264.7 cells (n=3 for each group). Cells were pretreated with AA13 for 30 min, followed by LPS (1 μg/mL) stimulation for 1 h. The translocation of p65 subunit of NF-κB was determined by immunochemistry.

measured. As shown in Figure 9B, AA13 (20 mg/kg) and antifani (10 mg/kg) significantly reduced the weight of the ear treated by dimethylbenzene. The anti-inflammatory effect of AA13 was further confirmed by H&E staining, which was consistent with the ear weight. As shown in Figure 9A, the ears receiving dimethylbenzene alone were twice as thick as the normal control ears. Treatment with AA13 and antifani obviously alleviated the edema and dimethylbenzene-induced subcutaneous tissue damage, even though the anti-swelling effect of AA13 was weaker than that of antifani.

Discussion

In this study, sarsasapogenin-AA13, a derivative of sarsasapogenin, could significantly inhibit dimethylbenzene-induced ear edema in mice and reduce the LPS-induced production of NO and PGE_2 in RAW264.7 cells, which is consistent with its parent compound[24, 31].

It has been demonstrated that NO, the major catalytic product of iNOS during the inflammatory process[32], is the important inflammatory mediator that plays important roles in the process of inflammation[33]. As a signaling molecule, NO is involved in many physiological processes at low concentrations and contributes to organ damage in numerous severe inflammatory process at high concentrations[34]. NO is produced by NOS, and iNOS is expressed prevailingly in activated macrophages induced by pro-inflammatory cytokines[35]. In this study, AA13 obviously inhibited LPS-induced NO release and iNOS expression correspondingly in macrophages, indicating that AA13 reduced the release of NO through decreasing the expression of iNOS.

TNF-α can increase expression levels of COX-2 and iNOS[36]. Therefore, we evaluated the levels of the inflammatory factors TNF-α and MCP-1 and the effect of AA13 on those inflammatory factors after LPS stimulation. Similarly, AA13 markedly inhibited the increase of TNF-α induced by LPS, but had no effect on the increase of MCP-1. These results reveal that AA13 might affect the upstream signaling of TNF-α and iNOS.

PGE_2 is an active mediator of inflammation, which is one of the major components of arachidonic acid metabolism catalyzed by COX-2[37]. In our study, LPS markedly increased the level of PGE_2, and AA13 inhibited the production of PGE_2 in a dose-dependent manner. These results indicate that the inhibition effects of AA13 on NO and PGE_2 production might be related to the inhibition of iNOS and COX.

To exclude the cytotoxic effect-induced decrease of COX-2 and iNOS by AA13, we detected the cell viability of sarsasapogenin-AA13 treated RAW264.7 cells. Sarsasapogenin-AA13 had no effect on cell viability at the concentrations of 20, 15, 10, and 50 μmol/L. However, LPS-induced NO and PGE_2 production was significantly inhibited in a concentration-dependent manner after treatment with sarsasapogenin-AA13. These results further confirmed the anti-inflammatory effects of AA13.

MAPKs are a family of serine/threonine kinases activated

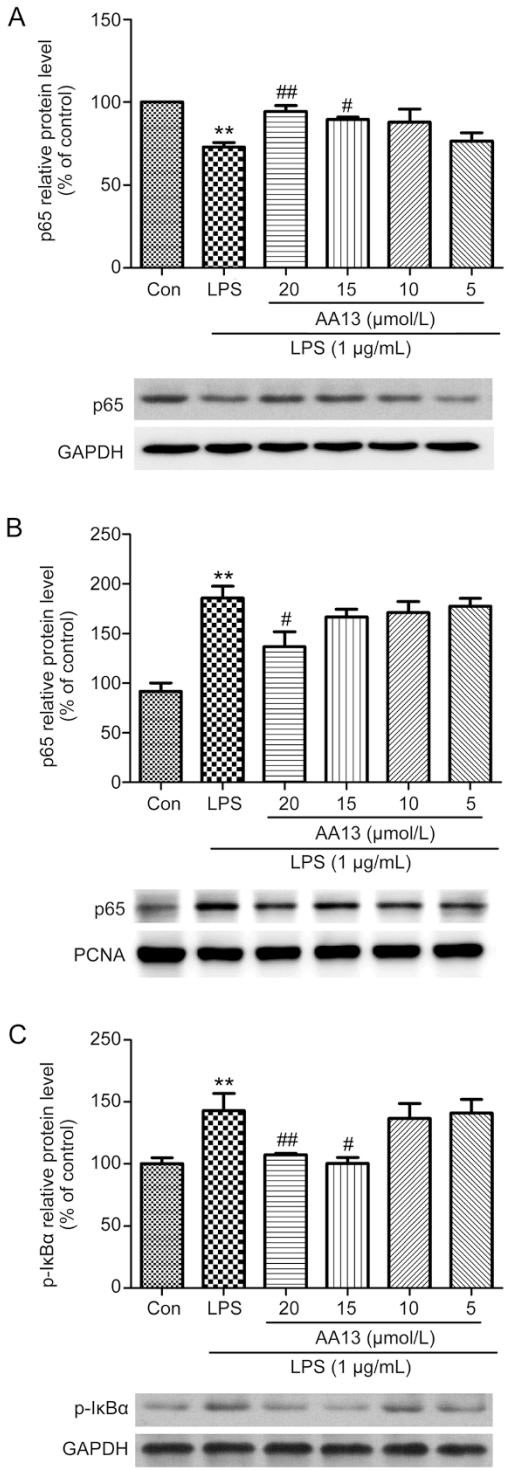

Figure 8. Effect of AA13 on LPS-stimulated NF-κB p65 translocation in RAW264.7 cells (n=3 for each group). Cells were pretreated with AA13 for 30 min, followed by LPS (1 μg/mL) stimulation for 1 h. Cytoplasmic (A) and nuclear (B) extracts were used to analyse p65 translocation by Western blot. GAPDH and PCNA were used as internal control to cytoplasmic and nuclear fractions. IκB phosphorylation (C) was measured to confirm the NF-κB activation. Mean±SEM. n=3 independent experiments. $^{**}P$<0.01 *vs* control group. $^{\#}P$<0.05, $^{\#\#}P$<0.01 *vs* LPS-stimulated group.

by diverse stimuli to mediate intracellular signaling and are associated with a variety of cellular activities[38]. It has been reported that the MAPKs signal pathway is related to the LPS-induced expression of COX-2 and iNOS[39, 40]. In this study, AA13 reduced the LPS-induced phosphorylation of p38 and JNK, but had no effect on the phosphorylation of ERK, though we did find that AA13 reduced the phosphorylation of ERK induced by hydrogen peroxide in SHSY5Y cells. These results suggested that the anti-inflammatory effect of AA13 was correlated with the MAPK signal pathway. However, the mechanism of how AA13 works on MAPK signaling needs further investigation.

The expression of inflammatory mediators is also modulated by NF-κB. Normally, inactive NF-κB is bound to IκB in the cytoplasm. Stimulated by LPS, IκB is phosphorylated, and NF-κB p65 moves from the cytoplasm to the nucleus to regulate the production of the inflammatory cytokines. The expression of many inflammation-related genes is regulated through the NF-κB signaling pathway[41]. The inhibition of NF-κB is initially considered important in the design of iNOS inhibitors[42]. As shown by our experiments, AA13 inhibited NF-κB transfer to the nucleus induced by LPS. Therefore, the results suggest that the inhibition of the phosphorylation of JNK and p38 and NF-κB activation may be involved in the inhibiting mechanism.

On the basis of the *in vitro* results, we examined the effect of AA13 on dimethylbenzene-induced ear edema in mice, which is a commonly used animal model for the preliminary screening of potential anti-inflammatory drugs[43]. Dimethylbenzene can induce the release of inflammatory mediators, and further cause acute edema. Using the model of ear edema, the anti-inflammatory effects of the compounds were found to inhibit LPS-induced inflammatory responses in RAW264.7 cells[43, 44]. Dai *et al* also reported that andrographolide derivatives, which alleviated the ear edema induced by dimethylbenzene, can reduce the level of iNOS and PGE_2 *in vivo*[45]. Thus, we hypothesized that AA13 may suppress the edema of the ear through inhibiting the releaseing of inflammatory factors and blocking the stimulating effect of inflammatory mediators. Our results based on the animal model demonstrated that AA13 possessed potential anti-inflammatory activity *in vivo*, which is consistent with a previous study.

In conclusion, our results indicate that AA13 modulated LPS-induced RAW264.7 cell activation for the first time. It significantly reduced the inflammatory factors, including NO, TNF-α and PGE_2, which was associated with its inhibition of NF-κB and MAPK signaling pathway activation; however, the target of AA13 is still vague (Figure 10). Accordingly, AA13 needs more comprehensive studies as a potential alternative in the treatment of inflammatory diseases that are associated with the over-activation of macrophages.

Acknowledgements

This project was supported by grants (to Rui WANG) from the National Natural Science Foundation of China (No 81072627),

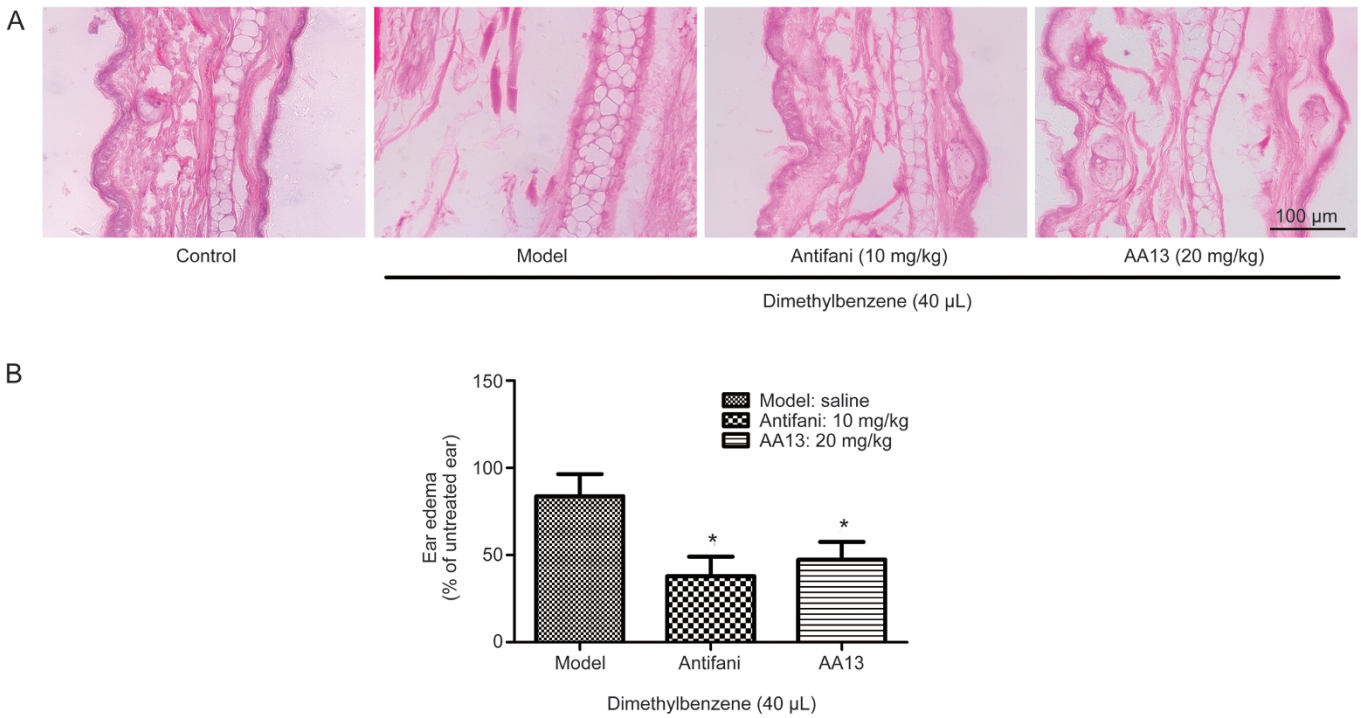

Figure 9. AA13 inhibited dimethylbenzene-induced ear edema in mice. Mice were randomly assigned into three groups: Model; Antifani (10 mg/kg) and AA13 (20 mg/kg). Dimethylbenzene was applied on inner and outer surface of right ears of mice to induce edema 1 h after the last drugs or vehicle administration. Histological alteration was detected by hematoxylin and eosin staining (A) and observed under microscope. Edema was determined as weight difference between the biopsies from right ear (dimethylbenzene treated) and the left ear (untreated control) (B). Mean±SEM. *n*=5 independent experiments. $^{*}P<0.05$ *vs* control group.

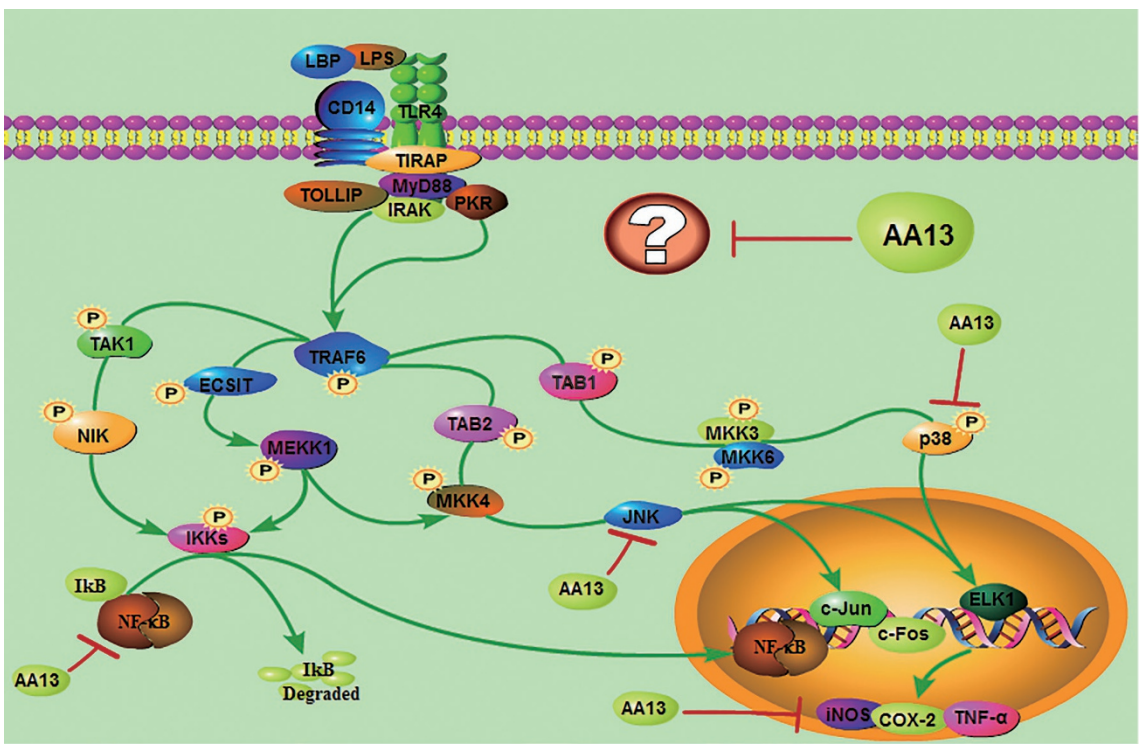

Figure 10. Inflammatory signaling pathways affected by AA13.

the 111 Project (No B07023) from the Ministry of Education, the Pujiang talent project (No 11PJ1402300), the Shanghai Biomedical Technology Support Program (No 15401901100), Shanghai Pujiang Program (15PJD012), and the Key project from Shanghai Science and Technology Committee (No 12431900901).

Author contribution

Rui WANG and Lei MA designed research; Dong DONG and Nan-nan ZHOU performed research; Jia-wei XIONG, Pan HUI and Lei MA contributed new analytical tools and reagents; Rui-xuan LIU and Si-qi SUN analyzed data; Dong DONG and Rui WANG wrote the paper.

References

1 Lundberg IE. The role of cytokines, chemokines, and adhesion molecules in the pathogenesis of idiopathic inflammatory myopathies. Curr Rheumatol Rep 2000; 2: 216–24.
2 Williams IR, Parkos CA. Colonic neutrophils in inflammatory bowel disease: double-edged swords of the innate immune system with protective and destructive capacity. Gastroenterology 2007; 133: 2049–52.
3 Mantovani A, Allavena P, Sica A, Balkwill F. Cancer-related inflammation. Nature 2008; 454: 436–44.
4 Glass CK, Saijo K, Winner B, Marchetto MC, Gage FH. Mechanisms underlying inflammation in neurodegeneration. Cell 2010; 140: 918–34.
5 Rochon YP, Frojmovic MM. A model for the recruitment of neutrophils at sites of inflammation. Physiological relevance of *in vivo* neutrophil aggregation. Med Hypotheses 1992; 38: 132–8.
6 Beutler B, Rietschel ET. Innate immune sensing and its roots: the story of endotoxin. Nat Rev Immunol 2003; 3: 169–76.
7 Li X, Kolltveit KM, Tronstad L, Olsen I. Systemic diseases caused by oral infection. Clin Microbiol Rev 2000; 13: 547–58.
8 Tilg H, Moschen AR, Kaser A. Suppression of interleukin-17 by type I interferons: a contributing factor in virus-induced immunosuppression? Eur Cytokine Netw 2009; 20: 1–6.
9 Abreu MT. The pathogenesis of inflammatory bowel disease: translational implications for clinicians. Curr Gastroenterol Rep 2002; 4: 481–9.
10 Aggarwal BB, Takada Y, Shishodia S, Gutierrez AM, Oommen OV, Ichikawa H, *et al.* Nuclear transcription factor NF-kappa B: role in biology and medicine. Indian J Exp Biol 2004; 42: 341–53.
11 Ahn KS, Aggarwal BB. Transcription factor NF-kappaB: a sensor for smoke and stress signals. Ann N Y Acad Sci 2005; 1056: 218–33.
12 Hayden MS, Ghosh S. Shared principles in NF-kappaB signaling. Cell 2008; 132: 344–62.
13 Blonska M, Lin X. NF-kappaB signaling pathways regulated by CARMA family of scaffold proteins. Cell Res 2011; 21: 55–70.
14 Park HJ, Kim IT, Won JH, Jeong SH, Park EY, Nam JH, *et al.* Anti-inflammatory activities of ent-16alphaH,17-hydroxy-kauran-19-oic acid isolated from the roots of *Siegesbeckia pubescens* are due to the inhibition of iNOS and COX-2 expression in RAW264.7 macrophages via NF-kappaB inactivation. Eur J Pharmacol 2007; 558: 185–93.
15 Kundu JK, Surh YJ. Breaking the relay in deregulated cellular signal transduction as a rationale for chemoprevention with anti-inflammatory phytochemicals. Mutat Res 2005; 591: 123–46.
16 Kishore R, McMullen MR, Cocuzzi E, Nagy LE. Lipopolysaccharide-mediated signal transduction: Stabilization of TNF-alpha mRNA contributes to increased lipopolysaccharide-stimulated TNF-alpha production by Kupffer cells after chronic ethanol feeding. Comp Hepatol 2004; 3: S31.
17 Suzuki T, Moraes TJ, Vachon E, Ginzberg HH, Huang TT, Matthay MA, *et al.* Proteinase-activated receptor-1 mediates elastase-induced apoptosis of human lung epithelial cells. Am J Respiratory Cell Mol Biol 2005; 33: 231–47.
18 Son Y, Cheong YK, Kim NH, Chung HT, Kang DG, Pae HO. Mitogen-activated protein kinases and reactive oxygen species: how can ROS activate MAPK pathways? J Signal Transduct 2011; 2011: 792639.
19 Liu YW, Zhu X, Lu Q, Wang JY, Li W, Wei YQ, *et al.* Total saponins from *Rhizoma Anemarrhenae* ameliorate diabetes-associated cognitive decline in rats: involvement of amyloid-beta decrease in brain. J Ethnopharmacol 2012; 139: 194–200.
20 Wang Y, Dan Y, Yang D, Hu Y, Zhang L, Zhang C, *et al.* The genus Anemarrhena Bunge: a review on ethnopharmacology, phytochemistry and pharmacology. J Ethnopharmacol 2014; 153: 42–60.
21 Hu Y, Xia Z, Sun Q, Orsi A, Rees D. A new approach to the pharmacological regulation of memory: Sarsasapogenin improves memory by elevating the low muscarinic acetylcholine receptor density in brains of memory-deficit rat models. Brain Res 2005; 1060: 26–39.
22 Hu H, Zhang R, Zhang Y, Xia Z, Hu Y. Role of CREB in the regulatory action of sarsasapogenin on muscarinic M1 receptor density during cell aging. FEBS Lett 2010; 584: 1549–52.
23 Lee B, Jung K, Kim DH. Timosaponin AIII, a saponin isolated from Anemarrhena asphodeloides, ameliorates learning and memory deficits in mice. Pharmacol Biochem Behavior 2009; 93: 121–7.
24 Kim JY, Shin JS, Ryu JH, Kim SY, Cho YW, Choi JH, *et al.* Anti-inflammatory effect of anemarsaponin B isolated from the rhizomes of Anemarrhena asphodeloides in LPS-induced RAW264.7 macrophages is mediated by negative regulation of the nuclear factor-kappaB and p38 pathways. Food Chem Toxicol 2009; 47: 1610–7.
25 Denizot F, Lang R. Rapid colorimetric assay for cell growth and survival. Modifications to the tetrazolium dye procedure giving improved sensitivity and reliability. J Immunol Methods 1986; 89: 271–7.
26 Guevara I, Iwanejko J, Dembinska-Kiec A, Pankiewicz J, Wanat A, Anna P, *et al.* Determination of nitrite/nitrate in human biological material by the simple Griess reaction. Clin Chim Acta 1998; 274: 177–88.
27 Noh EJ, Ahn KS, Shin EM, Jung SH, Kim YS. Inhibition of lipopolysaccharide-induced iNOS and COX-2 expression by dehydroevodiamine through suppression of NF-kappaB activation in RAW264.7 macrophages. Life Sci 2006; 79: 695–701.
28 Wang T, Wu F, Jin Z, Zhai Z, Wang Y, Tu B, *et al.* Plumbagin inhibits LPS-induced inflammation through the inactivation of the nuclear factor-kappa B and mitogen activated protein kinase signaling pathways in RAW264.7 cells. Food Chem Toxicol 2014; 64: 177–83.
29 Li X, Liu Y, Wang L, Li Z, Ma X. Unfractionated heparin attenuates LPS-induced IL-8 secretion via PI3K/Akt/NF-kappaB signaling pathway in human endothelial cells. Immunobiology 2015; 220: 399–405.
30 Lee HJ, Li H, Chang HR, Jung H, Lee da Y, Ryu JH. (–)-Nyasol, isolated from Anemarrhena asphodeloides suppresses neuroinflammatory response through the inhibition of I-kappaBalpha degradation in LPS-stimulated BV-2 microglial cells. J Enzyme Inhib Med Chem 2013; 28: 954–9.
31 Jiang Y, Yu L, Wang MH. N-*trans*-feruloyltyramine inhibits LPS-induced NO and PGE_2 production in RAW264.7 macrophages: Involvement of AP-1 and MAP kinase signalling pathways. Chem Biol Interact 2015; 235: 56–62.
32 Posadas I, Terencio MC, Guillen I, Ferrandiz ML, Coloma J, Paya M, *et al.* Co-regulation between cyclo-oxygenase-2 and inducible nitric oxide synthase expression in the time-course of murine inflammation.

Naunyn-Schmiedeberg's Arch Pharmacol 2000; 361: 98–106.
33 Cui Y, Kim DS, Park SH, Yoon JA, Kim SK, Kwon SB*, et al.* Involvement of ERK AND p38 MAP kinase in AAPH-induced COX-2 expression in HaCaT cells. Chem Physics Lipids 2004; 129: 43–52.
34 Boger RH. The *L*-arginine-nitric oxide pathway: Role as an antioxidant mechanism in atherosclerosis. Roy Soc Ch 1999; (240): 46–51.
35 Regunathan S, Piletz JE. Regulation of inducible nitric oxide synthase and agmatine synthesis in macrophages and astrocytes. Ann Ny Acad Sci 2003; 1009: 20–9.
36 Bertolini A, Ottani A, Sandrini M. Dual acting anti-inflammatory drugs: a reappraisal. Pharmacol Res 2001; 44: 437–50.
37 Marnett LJ, Rowlinson SW, Goodwin DC, Kalgutkar AS, Lanzo CA. Arachidonic acid oxygenation by COX-1 and COX-2 — mechanisms of catalysis and inhibition. J Biol Chem 1999; 274: 22903–6.
38 Huang PY, Han JH, Hui LJ. MAPK signaling in inflammation-associated cancer development. Protein Cell 2010; 1: 218–26.
39 Kaminska B. MAPK signalling pathways as molecular targets for anti-inflammatory therapy — from molecular mechanisms to therapeutic benefits. Biochim Biophys Acta 2005; 1754: 253–62.
40 Liu S, Jia H, Hou S, Zhang G, Xin T, Li H*, et al.* Recombinant TB10.4 of Mycobacterium bovis induces cytokine production in RAW264.7 macrophages through activation of the MAPK and NF-kappaB pathways via TLR2. Mol Immunol 2014; 62: 227–34.
41 Kanke T, Macfarlane SR, Seatter MJ, Davenport E, Paul A, McKenzie RC*, et al.* Proteinase-activated receptor-2-mediated activation of stress-activated protein kinases and inhibitory kappa B kinases in NCTC 2544 keratinocytes. J Biol Chem 2001; 276: 31657–66.
42 Aktan F. iNOS-mediated nitric oxide production and its regulation. Life Sci 2004; 75: 639–53.
43 Li Q, Yang S, Yang S, Xin F, Wang M. Anti-inflammatory activity of phlomisoside F isolated from Phlomis younghusbandii Mukerjee. Int Immunopharmacol 2015; 28: 724–30.
44 Zhao Z, Xiao J, Wang J, Dong W, Peng Z, An D. Anti-inflammatory effects of novel sinomenine derivatives. Int Immunopharmacol 2015; 29: 354–60.
45 Dai GF, Zhao J, Jiang ZW, Zhu LP, Xu HW, Ma WY*, et al.* Anti-inflammatory effect of novel andrographolide derivatives through inhibition of NO and PGE_2 production. Int Immunopharmacol 2011; 11: 2144–9.